

Self-assembly of Birnessite Manganese Dioxide into Monodisperse Honeycomb and Hollow Nanospheres

Hongmin Chen and Junhui He*

Functional Nanomaterials Laboratory, Technical Institute of Physics and Chemistry,
Chinese Academy of Sciences (CAS), Zhongguancun Beiyitiao 2, Haidianqu, Beijing 100080, P. R. China

(Received September 27, 2006; CL-061129; E-mail: jhhe@mail.ipc.ac.cn)

Monodisperse honeycomb and hollow nanospheres of ordered birnessite manganese dioxide nanoplatelets were facilely synthesized in high yields via the redox reaction of KMnO_4 and oleic acid and following self-assembly of produced nanoplatelets.

Manganese oxides have recently attracted much attention because of their ion-exchange and molecular adsorption¹ and catalytic,² electrochemical,³ and magnetic properties.⁴ Among them, birnessite type manganese dioxide (abbreviated as BirMnO_2) has a two-dimensional layered structure with edge-shared MnO_6 octahedra with cations and water molecules situated between the negatively charged layers. The interlayer spacing ranges from 0.69 to 0.7 nm.⁵ Natural BirMnO_2 exists widely in ores, soils, and deep-sea nodules. It can also be synthesized by oxidation of Mn^{2+} , reduction of MnO_4^- , and redox reactions between Mn^{2+} and MnO_4^- .⁶ BirMnO_2 has shown potential applications as heterogeneous catalysts in the reduction of NO , HCHO , Cr^{3+} , and AsO_3^{2-} ,⁷ oxidation of CO ,⁸ hydrogenation of alkenes,⁹ oxidation degradation of organic and inorganic contaminants,¹⁰ as adsorbents for nuclear wastes,¹¹ and as cathode¹² and magnetic⁴ materials. Assembly of transition-metal oxide nanoparticles into ordered structures such as hollow nanospheres is additionally interesting and highly desirable, as these structures may be used as catalysts, drug carriers, fillers, and photonic crystals. Very recently, Suib and co-workers reported the self-assembly of microporous $\gamma\text{-MnO}_2$ molecular sieve flakes into mesoporous hollow nanospheres that preliminarily showed enhanced catalytic activity and selectivity compared to the standard $\gamma\text{-MnO}_2$.² In the current communication, we reported a facile approach to synthesis of honeycomb and hollow BirMnO_2 nanospheres, which, to the best of our knowledge, has not yet been reported so far.

In a typical procedure, 0.10 g (0.63 mmol) of KMnO_4 was dissolved in 50 mL of pure water. After the mixture was stirred for ca. 10 min, 1 mL (3.2 mmol) of oleic acid (OA) was added. The mixture was maintained at room temperature for a certain period of time. A brown-black powder was collected, washed several times with pure water and alcohol, respectively, and dried in a vacuum at 60 °C for 10 h. The molar ratio of KMnO_4/OA was varied from 1:5 to 2:1. Under otherwise identical conditions, the yields of BirMnO_2 all exceeded 90%.

The products were characterized by X-ray powder diffraction (XRD), scanning (SEM) and transmission (TEM) electron microscopy, energy dispersive spectroscopy (EDS).¹³ XRD peaks were recorded at $2\theta = 12.29, 18.68, 36.84, 54.98$, and 65.76° and could be assigned to the (002), (101), (006), (301), and (119) planes of hexagonal BirMnO_2 (JCPDS 18-802). From $2\theta = 12.29^\circ$, the interlayer spacing was estimated to be ca.

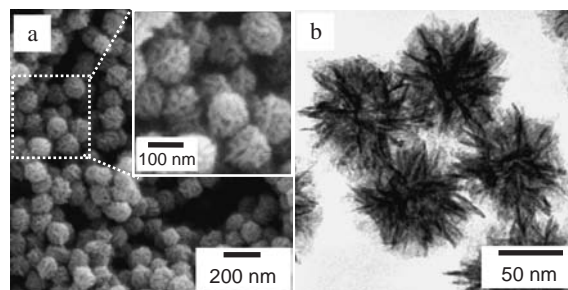


Figure 1. SEM (a) and TEM (b) images of honeycomb BirMnO_2 nanospheres ($\text{KMnO}_4/\text{OA} = 1:5$).

0.72 nm, in good agreement with the literature. Estimation by the Scherrer equation showed that the lamellar structure of BirMnO_2 has a thickness of ca. 8.1 nm.¹³ Thus, it is supposed to consist of ca. 7 layers. EDS results confirmed the presence of major Mn and O elements and minor K element.

Figure 1a shows a typical SEM image of the product obtained using a KMnO_4/OA ratio of 1:5 after redox reaction for 20 h. Clearly, the product consists of monodisperse nanospheres of ca. 97 nm in diameter. A magnified image (inset of Figure 1a) shows that the nanosphere in fact has a honeycomb structure that was formed by the assembly of nanoscale platelets. The thickness of such platelets was estimated to be ca. 10.7 nm, in agreement with the above XRD results. Figure 1b shows a typical TEM image of the nanospheres. Gray parts are platelets that were vertical to electron beam, and dark parts are those that were parallel to electron beam. Clearly, each nanosphere consists of platelets that join together at its center.

The size and morphology evolution of honeycomb MnO_2 nanospheres were studied by varying the reaction time (Figure 2). TEM images were recorded after redox reaction for 0.5, 2, 5, and 20 h, respectively. The initial nanostructure (0.5 h) has a diameter of ca. 50 nm and consists of nanoplatelets of ca. 2.2 nm in thickness. With increase of reaction time, the diameter of the nanostructure and the thickness of the nanoplatelet increased nearly to 75 and 3.0 nm (2 h), 83 and 3.3 nm (5 h), 89 and 5.2 nm (20 h), respectively. Thus, they are dependent on the redox reaction time. Another interesting observation was that the lamellar platelets initially looked very soft and foldable.¹⁴

Figures 3a and 3b show SEM and TEM images of the product obtained using a KMnO_4/OA ratio of 1:1 after redox reaction for 5 h. The clear contrast between the dark edge and the gray center of each nanosphere (Figure 3b) is evidence of its hollow nature. A close look at the shells shows that they consist of shorter and thinner platelets than the above honeycomb BirMnO_2 nanospheres. Their size distribution is also not as uniform as that of the latter. It is very interesting that both the

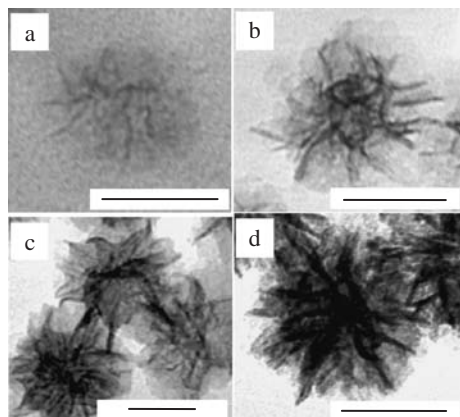


Figure 2. TEM images of honeycomb MnO_2 nanospheres obtained after different redox times: 0.5 (a), 2 (b), 5 (c), and 20 h (d), respectively. Scale bar: 50 nm.

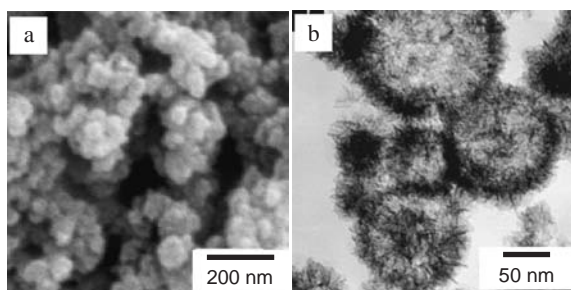
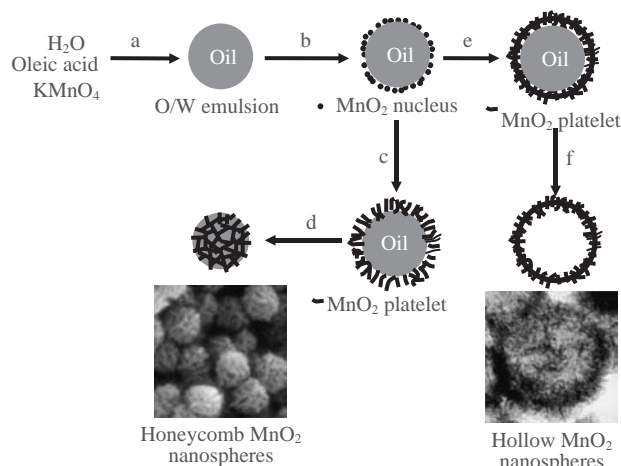


Figure 3. SEM (a) and TEM (b) images of hollow MnO_2 nanospheres ($\text{KMnO}_4/\text{OA} = 1:1$).

honeycomb and hollow BirMnO_2 nanospheres had no changes in morphology upon ultrasonic treatment (120 W) for 30 min, indicating the robustness of the nanospheres.

Based on the above results, a plausible mechanism was proposed and is shown in Scheme 1. Oleic acid has a hydrophilic carboxyl head group and a hydrophobic alkene chain, which can form a stable O/W emulsion at appropriate concentrations (Process a). In the emulsion, the reaction quickly occurs between KMnO_4 and oleic acid at the O/W interface and produces MnO_2 nuclei there (Process b). At low KMnO_4 concentrations, small amounts of lamellar MnO_2 nanoplatelets are produced and organized along the radius direction, and thus an unstable shell of loosely packed nanoplatelets is formed (Process c). Removal of oleic acid and formed *cis*-diol by rinsing with ethanol results in collapse of the shell, giving ordered honeycomb nanostructures (Process d). In contrast, large amounts of lamellar nanoplatelets are produced and densely packed with each other at high KMnO_4 concentrations. Thus, a robust BirMnO_2 shell is formed (Process e), which is self-supporting even after removal of oleic acid and formed *cis*-diol. Eventually, hollow nanospheres are formed (Process f).

In summary, a novel approach to preparation of BirMnO_2 nanostructures was developed. It involves a redox reaction of KMnO_4 and oleic acid at the O/W interface, followed by self-assembly of formed BirMnO_2 nanoplatelets into BirMnO_2 nanostructures. Both monodisperse honeycomb and hollow BirMnO_2 nanospheres were prepared at room temperature in high yields depending on the molar ratio of KMnO_4/OA . Nitro-



Scheme 1. Plausible formation mechanisms of honeycomb and hollow BirMnO_2 nanospheres.

gen absorption-desorption measurements showed that these BirMnO_2 nanostructures have mesoporous structures that are assembled from lamellar nanoplatelets. Such unique nanostructures may have enhanced physicochemical properties such as enhanced electrochemical properties and catalytic activity in oxidative degradation of contaminants.^{7,10,11}

This work was supported by the National Natural Science Foundation of China (Grant No. 20471065), the Hundred Talents Program and the President Fund of CAS.

References

- 1 L. Al-Attar, A. Dyer, R. Harjula, *J. Mater. Chem.* **2003**, *13*, 2963.
- 2 J. Yuan, K. Laubernds, Q. Zhang, S. L. Suib, *J. Am. Chem. Soc.* **2003**, *125*, 4966; L. Z. Wang, Y. Ebina, K. Takada, T. Sasaki, *Chem. Commun.* **2004**, 1074.
- 3 M. Nakayama, S. Konishi, H. Tagashira, K. Ogura, *Langmuir* **2005**, *21*, 354.
- 4 J. Ge, L. Zhuo, F. Yang, B. Tang, L. Zhu, C. Tung, *J. Phys. Chem. B* **2006**, *110*, 17854.
- 5 Q. Feng, H. Kanoh, K. Ooi, *J. Mater. Chem.* **1999**, *9*, 319.
- 6 Y. H. Xu, Q. Feng, K. Kajiyoshi, K. Yanagisawa, *Chem. Mater.* **2002**, *14*, 697; A. C. Gaillot, B. Lanson, V. A. Drits, *Chem. Mater.* **2005**, *17*, 2959; Y. Omomo, T. Sasaki, L. Wang, M. Watanabe, *J. Am. Chem. Soc.* **2003**, *125*, 3568.
- 7 Y. Sekine, *Atmos. Environ.* **2002**, *36*, 5543.
- 8 A. L. Cabrera, M. B. Maple, G. Arrhenius, *Appl. Catal.* **1990**, *64*, 309.
- 9 M. Nitta, *Appl. Catal.* **1984**, *9*, 151.
- 10 K. A. Barrett, M. B. McBride, *Environ. Sci. Technol.* **2005**, *39*, 9223; L. E. Power, Y. Arai, D. L. Sparks, *Environ. Sci. Technol.* **2005**, *39*, 181.
- 11 Q. Feng, H. Kanoh, Y. Miyai, K. Ooi, *Chem. Mater.* **1995**, *7*, 1226.
- 12 M. S. El-Deab, T. Ohsaka, *Angew. Chem., Int. Ed.* **2006**, *45*, 5963.
- 13 See Supporting Information. Supporting Information is also available electronically on the CSJ-Journal Web site, <http://www.csj.jp/journals/chem-lett/index.html>.
- 14 J. He, T. Kunitake, *Soft Matter* **2006**, *2*, 119.